

# Lithium and lithium-carbon isoelectronic complexes in silicon: Luminescence-decay-time, absorption, isotope-splitting, and Zeeman measurements

E. C. Lightowers, L. T. Canham, and G. Davies

*Physics Department, King's College, University of London, Strand, London WC2R 2LS, United Kingdom*

M. L. W. Thewalt and S. P. Watkins

*Department of Physics, Simon Fraser University, Burnaby, British Columbia, Canada V5A 1S6*

(Received 28 November 1983)

Irradiation damage in lithium-doped silicon gives rise to the well-known  $Q$  luminescence-absorption system with no-phonon lines at  $\sim 1.045$  eV. In irradiated lithium-doped material with a high carbon concentration a second luminescence-absorption system is also prominent at higher energy, the  $S$  system with no-phonon lines at  $\sim 1.082$  eV. Isotope-splitting data on the no-phonon lines indicate that the  $S$  optical center, like the  $Q$  center, contains four lithium atoms, but with a near-neighbor carbon atom. Luminescence-decay-time measurements confirm that in both cases the luminescence may be identified with exciton decay at neutral isoelectronic centers and, together with absorption measurements, yield approximate values for the defect concentrations. Zeeman measurements on the  $Q$  system show that of the three no-phonon lines observed at zero stress, the higher-energy lines are magnetic singlets and that the lowest-energy line is an isotropic spin triplet.

## I. INTRODUCTION

Irradiation damage in lithium-doped silicon gives rise to a vibronic luminescence-absorption system with three thermalizing no-phonon lines at  $\sim 1.045$  eV [Fig. 1(a)]. Isotope substitution and uniaxial stress measurements have shown that the optical center responsible contains four lithium atoms and has a trigonal distortion. It has been proposed that the four lithium atoms replace a single silicon atom at a substitutional site to produce an axial molecular isoelectronic trap.<sup>1</sup> Efficient luminescence is produced by electron-hole recombination in an exciton bound at this neutral center. Exciton decay at several other axial isoelectronic traps in silicon has recently been reported,<sup>2-4</sup> but only in one other case, the beryllium-pair complex, have the chemical constituents and structure of the optical center been unambiguously identified.<sup>3,4</sup> A detailed account of isoelectronic centers in other semiconductors, in particular GaP, has been given by Dean and Herbert.<sup>5</sup>

In this paper we describe luminescence-decay-time measurements which confirm the isoelectronic nature of the optical center, and from these data and optical-absorption measurements an estimate is made of the concentration. Preliminary Zeeman results are also reported which indicate that the energy-level structure differs significantly from that proposed by Morgan and Morgan,<sup>6</sup> which is commonly used to describe axial isoelectronic centers, and has more in common with that recently employed to describe antimony- and copper-related isoelectronic complexes in GaP.<sup>7</sup>

In an earlier paper<sup>8</sup> it was reported that a similar but very much weaker luminescence system, the  $S$  system with no-phonon lines  $\sim 1.082$  eV [Fig. 1(b)], always accompanied the 1.045-eV  $Q$  system in 2-MeV electron-irradiated lithium-doped silicon, with a no-phonon  $Q$ -

$S$ -line intensity ratio varying between 5 and 100. The ratio is dependent on the starting material, lithium concentration, radiation dose, and subsequent thermal treatment. Most of the previous work on the  $Q$  system has been carried out using high-purity float-zone silicon as starting material, with carbon and oxygen concentrations  $\leq 10^{15}$  cm<sup>-3</sup> compared with a lithium concentration of  $\sim 10^{17}$  cm<sup>-3</sup> introduced by diffusion. In this paper we show that the  $S$  system is considerably enhanced in float-zone silicon with a high carbon concentration, especially following suitable annealing treatment. Luminescence-decay-time measurements show that the  $S$  optical center is also an isoelectronic trap, and isotope structure in the no-phonon line with relative concentrations  $[^6\text{Li}]/[^7\text{Li}] \sim 0.5$  indicates that this center contains four lithium atoms. We therefore identify the  $S$  system with a four-lithium-atom complex replacing a substitutional silicon atom with a near-neighbor carbon atom. Recent work has also confirmed the suggestion by Thewalt *et al.*<sup>4</sup> that the higher-energy luminescence system which accompanies beryllium-pair luminescence is a beryllium-pair complex with a nearest-neighbor carbon atom.<sup>9</sup>

## II. EXPERIMENTAL

Samples for investigating the  $Q$  system were prepared from 20-k $\Omega$  cm float-zone silicon (Hoboken) with a carbon concentration  $\leq 10^{15}$  cm<sup>-3</sup> and an oxygen concentration  $\leq 10^{14}$  cm<sup>-3</sup>. The optimum conditions for maximizing the  $S$  system were obtained in 24- $\Omega$  cm float-zone material specifically doped with  $1.7 \times 10^{17}$  cm<sup>-3</sup> carbon and containing  $< 10^{16}$  cm<sup>-3</sup> oxygen (Mullard Southampton). In samples 1–2 mm thick, a doping level of  $\sim 1.5 \times 10^{17}$  cm<sup>-3</sup> electrically active natural lithium was obtained using a variation of the technique described by Pell.<sup>10</sup> The samples were lightly painted on both sides with a suspen-

sion of lithium in mineral oil, placed in a tantalum container in a quartz tube, and heated in a stream of helium. After heating for 30 min at 200°C to drive off the oil, the temperature was raised to 550°C for a further period of 30 min to drive in the lithium. Excess lithium was then re-

moved by a rinse in deionized water and the samples were heated for another 2 h at 600°C to produce an even distribution of the lithium. For mixed isotope doping at a similar concentration, a preprepared mixture of natural lithium (92.6 wt. %  $^7\text{Li}$ ) and isotopically enriched material (95 wt. %  $^6\text{Li}$ ) was evaporated onto one surface of the sample which was then heated in vacuum in the evaporation chamber at  $\sim 700^\circ\text{C}$  for 2 h.

The samples were irradiated at room temperature, on one side for thicknesses of  $\sim 1$  mm or on both sides for a thickness of  $\sim 2$  mm, with  $\sim 10^{17}\text{-cm}^{-2}$  2-MeV electrons. Luminescence spectra were recorded with the samples freely suspended in liquid helium at 4.2 K or with the helium pumped just below the  $\lambda$  point. The luminescence was excited by the combined red lines of a Kr laser, analyzed by a  $\frac{3}{4}$ -m Spex monochromator fitted with a 600-groove/mm grating blazed at  $1.2\ \mu\text{m}$ , and detected by a North Coast EO-817 Ge detector. The luminescence spectra were corrected for the system response by measuring the spectrum and temperature of a tungsten strip lamp, taking into account the variation of the emissivity of tungsten with wavelength. The absorption data were obtained with a similar monochromator and detector using a high-stability tungsten strip lamp as a source. The monochromator and most of the optical path were flushed with dry nitrogen to reduce atmospheric water-vapor absorption in the (1.05–1.10)-eV spectral region. The Zeeman measurements were carried out in the Voigt configuration with the sample suspended in the variable-temperature enclosure of an Oxford Instruments SpectroMag superconducting magnet.

The luminescence-decay-time measurements were obtained with the sample suspended in liquid helium, for temperatures at and below 4.2 K, or mounted in indium on the temperature-controlled block of a Vari-Temp Dewar for higher temperatures. Excitation pulses were provided by mechanically chopping the output of an Ar laser at 514.5 nm, and the luminescence was analyzed by a  $\frac{3}{4}$ -m double monochromator and detected by a Varian Associates VPM-159 A3 photomultiplier. The output of the photomultiplier was analyzed with a multichannel scaler.

### III. RESULTS AND DISCUSSION

#### A. General features of the $Q$ and $S$ luminescence and absorption

The luminescence spectrum in Fig. 1(a) shows the two lower-energy no-phonon lines and the one-phonon sideband of the  $Q$  system. The features labeled  $A$ ,  $B$ , and  $C$  are due to in-band resonance modes of the center and have been discussed elsewhere.<sup>1,8,11</sup> The sharp lines between 1.02 and 1.03 eV are specimen dependent and are not associated with the  $Q$  system. The insets show the no-phonon lines in greater detail. The strongest component of each line is due to centers containing four  $^7\text{Li}$  atoms and the structure at lower energies is associated primarily with centers containing three  $^7\text{Li}$  atoms and one  $^6\text{Li}$  atom.<sup>1</sup> There is a large change in the relative intensity of the  $Q$  and  $Q_L$  lines between 2.1 and 4.2 K. In a previous study<sup>11</sup> they have been shown to thermalize with an activation en-

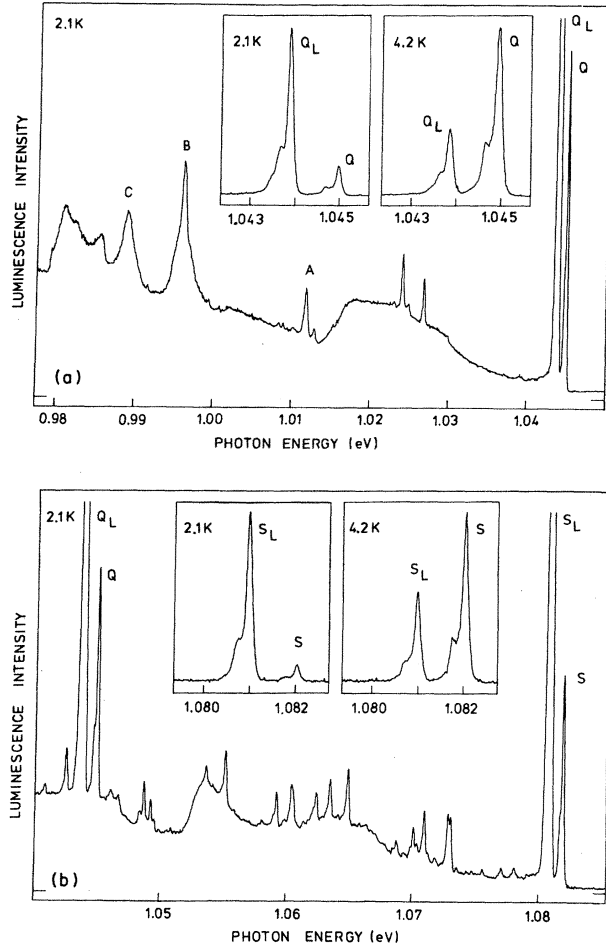


FIG. 1. Luminescence spectra excited by the combined red lines of a Kr laser with a power of 200 mW at the bath temperatures indicated, corrected for the transfer function of the monochromator and detector. The ordinate axis is proportional to photons per unit energy interval. The samples were diffused with  $\sim 1.5 \times 10^{17}\text{ cm}^{-3}$  natural lithium (92.6 wt. %  $^7\text{Li}$ ) and irradiated at room temperature with  $\sim 10^{17}\text{-cm}^{-2}$  2-MeV electrons. (a) Starting material was high-purity float-zone silicon with a carbon concentration  $\leq 10^{15}\text{ cm}^{-3}$  and an oxygen concentration  $\leq 10^{14}\text{ cm}^{-3}$ . The insets show the thermalization of the  $Q$  and  $Q_L$  no-phonon lines; the higher-energy  $Q_H$  component (Fig. 2) is not observed at  $\leq 4.2$  K. The features labeled  $A$ ,  $B$ , and  $C$  are due to in-band resonance modes of the center (Refs. 1 and 8). The lines between 1.02 and 1.03 eV are not related to the  $Q$  system. (b) Starting material was float-zone silicon with a carbon concentration of  $1.7 \times 10^{17}\text{ cm}^{-3}$  and with an oxygen concentration  $< 10^{16}\text{ cm}^{-3}$ . The sample was annealed for 1 h at 300°C after irradiation. The insets show the thermalization of the  $S$  and  $S_L$  no-phonon lines; the higher-energy  $S_H$  and  $S^*$  components (Fig. 2) are not observed at  $\leq 4.2$  K. The lines on the one-phonon sideband are not related to the  $S$  system.

ergy of  $1.07 \pm 0.05$  meV, which is equal to the spectroscopic splitting, and the projected no-phonon  $Q$ - to  $Q_L$ -line ratio at infinite temperature is  $45 \pm 5$ . Measurements on a number of samples with different doping levels have shown that the no-phonon  $Q$ - to  $Q_L$ -line ratio at 4.2 K is specimen independent.

The luminescence spectrum in Fig. 1(b) shows the two lowest-energy no-phonon lines and the acoustic branch of the one-phonon sideband for the  $S$  system. No in-band resonances have been identified for the  $S$  system and the lines on the phonon wing are dependent on the starting

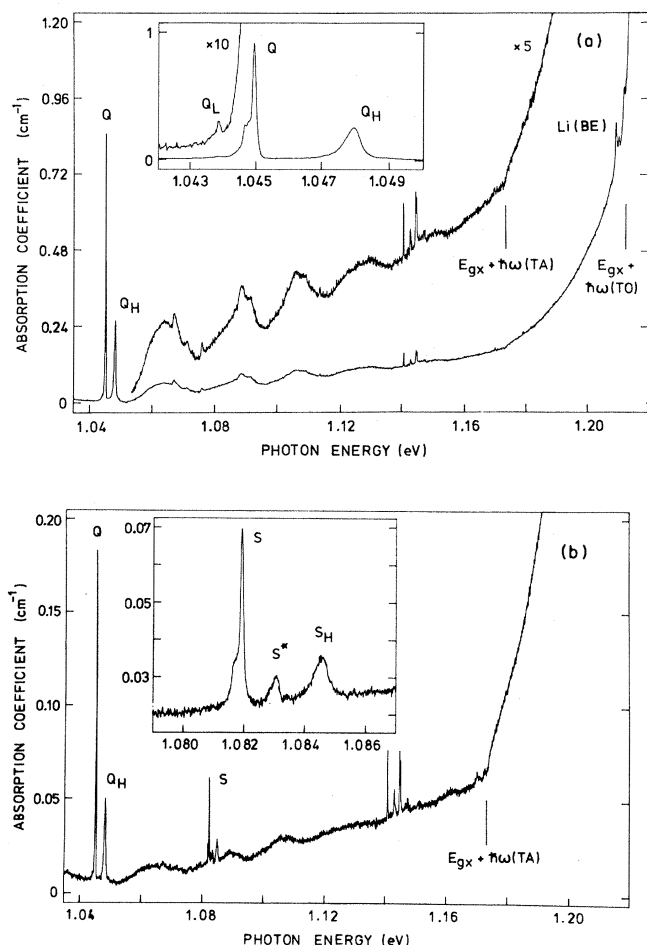


FIG. 2. Absorption spectra associated with the creation of excitons bound to the  $Q$  and  $S$  optical centers recorded at 2.1 K. The absorption edges due to the TA- and TO-phonon-assisted creation of free excitons are indicated together with structure [Li(BE)] due to the creation of excitons bound to neutral lithium donors. The sharp lines near 1.145 eV are not associated with the  $Q$  and  $S$  centers. (a) Sample measuring  $14 \times 6 \times 2$  mm<sup>3</sup> was cut from high-purity float-zone silicon diffused with  $4 \times 10^{17}$  cm<sup>-3</sup> natural lithium and irradiated on both sides with  $\sim 2 \times 10^{17}$ -cm<sup>-2</sup> 2-MeV electrons. (b) Sample measuring  $20 \times 6 \times 2$  mm<sup>3</sup> was cut from float-zone silicon containing  $1.7 \times 10^{17}$  cm<sup>-3</sup> carbon, diffused with  $1.5 \times 10^{17}$  cm<sup>-3</sup> natural lithium and irradiated on both sides with  $\sim 1 \times 10^{17}$  cm<sup>-3</sup> 2-MeV electrons.

material, the lithium-doping level, the radiation dose, and subsequent thermal treatment.<sup>12</sup> In this sample, which had a carbon concentration of  $1.7 \times 10^{17}$  cm<sup>-3</sup>, a lithium concentration of  $1.5 \times 10^{17}$  cm<sup>-3</sup>, and which was annealed for 1 h at 300°C after an irradiation dose of  $\sim 1 \times 10^{17}$ -cm<sup>-2</sup> 2-MeV electrons, the intensities of the  $S$  and  $Q$  no-phonon lines are approximately equal. From a comparison of the insets in Figs. 1(b) and 1(a) it can be seen that the no-phonon line isotope structure is very similar for the  $S$  and the  $Q$  lines. Preliminary measurements indicate that the  $S$  and  $S_L$  thermalize with an activation energy of  $1.00 \pm 0.05$  meV with an infinite temperature ratio of  $I_S/I_{S_L} = 32 \pm 5$ .<sup>12</sup>

Absorption data for the  $Q$  and  $S$  centers are shown in Fig. 2. Figure 2(a) was obtained with a 15-mm path length in a 2-mm thick sample prepared from high-purity float-zone material doped with  $4 \times 10^{17}$  cm<sup>-3</sup> lithium (drive-in temperature of 580°C) and irradiated on both sides with  $\sim 2 \times 10^{17}$ -cm<sup>-2</sup> 2-MeV electrons. The two higher-energy no-phonon lines are dominant in absorption with  $I_Q/I_{Q_H} = 1.32 \pm 0.03$ , and  $I_Q/I_{Q_L}$  lying between 50 and 100, depending on how the underlying background is

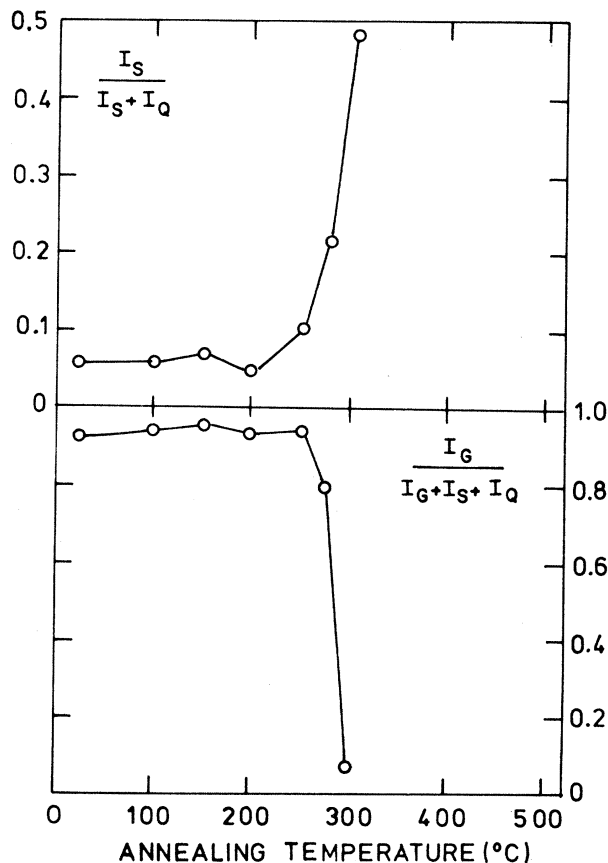


FIG. 3. Isochronal annealing data for a sample containing  $1.7 \times 10^{17}$  cm<sup>-3</sup> carbon and  $7 \times 10^{15}$  cm<sup>-3</sup> lithium irradiated with  $\sim 3 \times 10^{16}$ -cm<sup>-2</sup> 2-MeV electrons. The relative intensities of the  $S$ ,  $Q$  and the carbon-related 0.969-eV  $G$  no-phonon lines, measured in luminescence at 4.2 K, are plotted as a function of annealing temperature. The annealing times were 20 min.

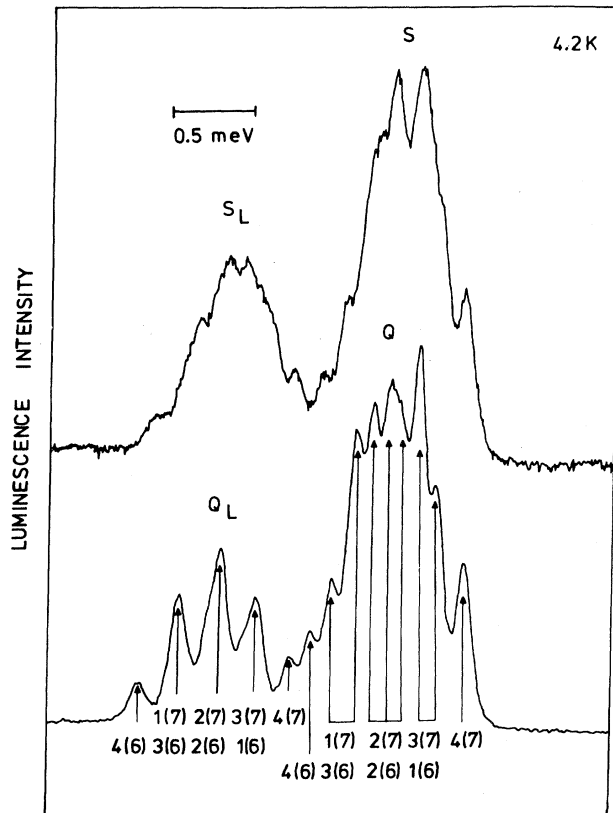


FIG. 4. Luminescence spectra of the  $Q$  and  $S$  no-phonon lines recorded at 4.2 K for a float-zone sample containing  $1.7 \times 10^{17} \text{ cm}^{-3}$  carbon diffused with  $\sim 7 \times 10^{17} \text{ cm}^{-3}$  lithium with  $[^6\text{Li}]/[^7\text{Li}] \leq 1$  and irradiated with  $\sim 2 \times 10^{17} \text{ cm}^{-2}$  2-MeV electrons. The structure in the  $Q$  lines is related to the isotopic composition of the centers in the lower part of the figure (Ref. 1).

interpreted in the inset of Fig. 2(a). The latter range is somewhat higher than the ratio of  $45 \pm 5$  determined from the luminescence data; the reason for this difference is not clear. The lines at  $\sim 1.145 \text{ eV}$  are specimen dependent, are not related to the  $Q$  or  $S$  systems, and have no counterparts in luminescence. The phonon sideband in absorption merges with the TA- and TO-phonon-assisted free-exciton absorption edges. The lines labeled Li(BE) are associated with the TO-phonon-assisted creation of excitons bound to isolated lithium donors.<sup>13</sup> The strength of these features indicates (Ref. 13 and assuming a TO-TA phonon-assisted ratio of  $\sim 20$ ) that the residual unaggregated lithium concentration is  $\sim 2 \times 10^{16} \text{ cm}^{-3}$ . This cannot be observed in luminescence, presumably because of the competition from other radiative and nonradiative processes.

Figure 2(b) shows the absorption obtained with a 20-mm path length in a 2-mm-thick sample containing  $1.7 \times 10^{17} \text{ cm}^{-3}$  carbon, doped with  $1.5 \times 10^{17}$  lithium, and irradiated on both sides with  $\sim 1 \times 10^{17} \text{ cm}^{-2}$  2-MeV electrons. The  $Q$  system is  $\sim 5 \times$  weaker than in the previous

sample and the no-phonon  $Q$ - to  $S$ -line ratio is  $\sim 3.8$ . There are four no-phonon lines for the  $S$  system and  $I_S/I_{S_H} = 1.65 \pm 0.05$  and  $I_S/I_{S^*} = 5.1 \pm 0.5$ . The  $S^*$  line is apparent in luminescence spectra obtained above 10 K. Neither the  $S_L$  line nor the phonon sideband of the  $S$  system have been detected in absorption.

### B. Isochronal annealing measurements

The data presented above strongly suggest that the  $S$  system may be associated with exciton decay at an isoelectronic complex containing both lithium and carbon. Further evidence is provided by the isochronal annealing data shown in Fig. 3. Room-temperature irradiation of carbon-doped silicon gives rise to a luminescence-absorption system with a no-phonon line at 0.969 eV (often referred to as the  $G$  line). This has been extensively studied and has been ascribed to a complex containing two carbon atoms and an interstitial silicon atom.<sup>14</sup> This is a major feature in irradiated material doped with both carbon and lithium and is the dominant luminescence system when the lithium concentration is very much less than the carbon concentration.

Figure 3 shows the effects of 20-min annealing stages up to  $300^\circ\text{C}$  on the relative intensities of the  $S$ ,  $Q$ , and  $G$  lines observed in luminescence at 4.2 K. The sample investigated contained  $1.7 \times 10^{17} \text{ cm}^{-3}$  carbon and  $7 \times 10^{15} \text{ cm}^{-3}$  Li (drive-in temperature  $400^\circ\text{C}$ ) and was irradiated with  $\sim 3 \times 10^{16} \text{ cm}^{-2}$  2-MeV electrons. It can be seen that the ratio  $I_S/I_Q$  increases from  $\sim 0.05$  to close to unity as the carbon-related  $G$  line anneals out. This suggests that carbon atoms liberated from the 0.969-eV optical centers can migrate to the  $Q$  centers and convert them into  $S$  centers. The effects of annealing are less dramatic when the carbon and lithium concentrations are comparable, but an increase in the ratio  $I_S/I_Q$  of the order of 2 or 3 has generally been obtained with a  $300^\circ\text{C}$  anneal. At higher temperatures the  $S$  and  $Q$  luminescence decreases and has completely disappeared by  $400^\circ\text{C}$  to be replaced by other luminescence systems.

### C. Isotope substitution

Several samples have been prepared containing the  $Q$  and  $S$  systems with comparable intensities and a range of  $[^6\text{Li}]/[^7\text{Li}]$  ratios. High-resolution spectra of the  $S$ ,  $S_L$ ,  $Q$ , and  $Q_L$  lines for a specimen with a  $[^6\text{Li}]/[^7\text{Li}]$  ratio close to, but slightly less than, unity, is shown in Fig. 4. The five major components in  $Q_L$  and the nine components in  $Q$  have been considered in detail by Canham *et al.*<sup>1</sup> and are consistent with a trigonally distorted optical center containing four lithium atoms. The identification of the components of  $Q$  and  $Q_L$  in terms of the isotopic structure of the different optical centers is indicated in the lower part of the figure.

Both the  $S$  and  $Q$  lines were obtained with the same spectral slit width but the structure in the  $S$  lines is not as well resolved as in the  $Q$  lines for reasons which are not understood. There is, however, a broad similarity between the structures of the  $S$  and  $Q$  lines with the suggestion of a possible reduction of the number of components at the center of the  $S$  line. For a four-lithium-atom complex

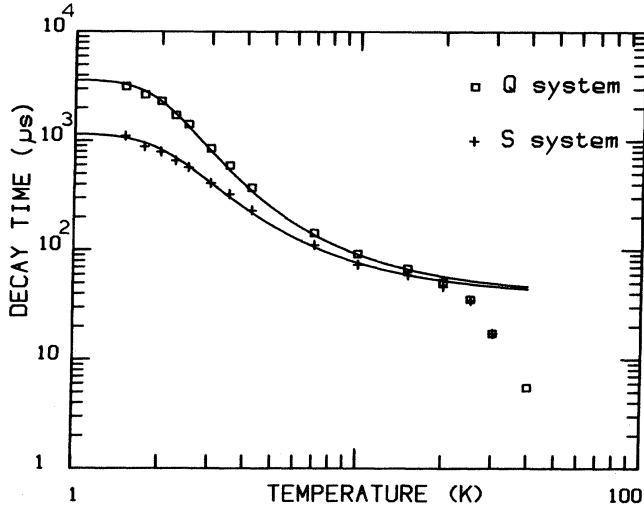


FIG. 5. Luminescence-decay times of the  $Q$  and  $S$  no-phonon lines are plotted as a function of temperature. The lines are theoretical fits to Eq. (1) yielding the parameters quoted in the text.

with trigonal symmetry the total number of components expected is eight, and the three components of  $Q$  for centers containing two  ${}^6\text{Li}$  and two  ${}^7\text{Li}$  atoms are considered to be due to the effect of the mixed isotopes upon lowering the symmetry from  $C_{3v}$ . With a neighboring carbon atom producing an axial perturbation, the symmetry lowering caused by the isotopes is likely to be less important. In contrast with  $Q_L$  and  $Q$ ,  $S_L$  appears to exhibit structure identical with  $S$ . A more detailed investigation over a range of accurately determined isotope ratios is required to provide a more complete explanation of the structure. However, the data in Fig. 4 appear to support a model for the  $S$  center as a modified  $Q$  center with a near-neighbor carbon atom.

#### D. Luminescence-decay-time measurements

Figure 5 shows a plot of the luminescence-decay time of the  $Q$  and  $S$  systems as a function of temperature. The very long decay times are characteristic of exciton decay at a neutral defect where there is no competition from nonradiative Auger processes. In the temperature range up to 15 K, where thermal ionization begins to be significant, the luminescence is almost entirely via the states responsible for the  $Q, Q_L$  and  $S, S_L$  lines with negligible contributions from higher levels. Hence the curves in Fig. 5 are theoretical fits to the decay time using the expression

$$\tau = \frac{1 + \frac{g_2}{g_1} \exp\left[-\frac{\Delta E}{kT}\right]}{\frac{1}{\tau_1} + \frac{g_2}{g_1 \tau_2} \exp\left[-\frac{\Delta E}{kT}\right]}, \quad (1)$$

where  $\tau$  is the calculated decay time,  $1/\tau_1$  and  $1/\tau_2$  are the recombination rates for the exciton in states responsible for the  $Q_L, S_L$ , and  $Q, S$  lines, respectively, with de-

generacies  $g_1$  and  $g_2$ , and  $\Delta E$  is the energy difference between these states.

Assuming  $g_2/g_1=1/3$  (see Sec. III E) the best fit for the  $Q$  system is obtained with  $\tau_{Q_L}=3600 \mu\text{s}$ ,  $\tau_Q=9.5 \mu\text{s}$ , and  $\Delta E_Q=0.93 \text{ meV}$ , and for the  $S$  system, the best fits obtained with  $\tau_{S_L}=1150 \mu\text{s}$ ,  $\tau_S=9.5 \mu\text{s}$ , and  $\Delta E_S=0.80 \text{ meV}$ . The values obtained for  $\Delta E$  are smaller than the observed spectroscopic splittings of 1.07 meV for the  $Q$  system and 1.00 meV for the  $S$  system, which is probably due to sample heating above the measured bath or cold-finger temperatures. However, making small adjustments to the temperature to force a fit for  $\Delta E$  does not significantly change the values obtained for  $\tau_1$  and  $\tau_2$ . Although the ratio  $g_2\tau_1/g_1\tau_2$  of 40 for the  $S$  system agrees reasonably well with the infinite-temperature ratio of the no-phonon lines  $I_S/I_{S_L}=32\pm 5$ , the value of 126 for the  $Q$  system is substantially higher than  $I_Q/I_{Q_L}=45\pm 5$  obtained in luminescence. This cannot be accounted for by the different phonon coupling of the higher- and lower-energy transitions. In the luminescence spectra in Fig. 1 it is difficult to ascertain the extent of any underlying background luminescence from other systems, but for the acoustic part of the phonon sideband this should be quite negligible. From measurements at 2.1 and 4.2 K it would appear that both the  $Q$  and  $S$  transitions are slightly more strongly coupled to acoustic phonons than the  $Q_L$  and  $S_L$  transitions, but the ratio of the area of the acoustic-mode sideband to the zero-phonon line is only  $\sim 25\%$  greater. Judging from the relative magnitude of the optical-phonon cutoff of the  $Q$  system at  $\sim 0.98 \text{ eV}$ , the coupling of the  $Q$  and  $Q_L$  transitions to the optic branch of the phonon spectrum does not differ significantly. The reason for the discrepancy between the lifetime and the no-phonon line intensities is not known.

If it is assumed that the  $Q$  and  $S$  centers deexcite entirely radiatively, the transition oscillator strengths, including the phonon sideband, are given in SI units by<sup>15</sup>

$$f = \frac{2\pi m^* \epsilon_0 c^3 \hbar^2}{n e^2 E^2 \tau} \frac{g_i}{g_f}, \quad (2)$$

where  $E$  is the transition energy,  $\tau$  is the radiative lifetime,  $g_i$  and  $g_f$  are the degeneracies of the initial and final states of the transition, and  $n$  is the refractive index. Substituting  $m^*=0.418m_0$  (appropriate for donors),  $n=3.5$ ,  $g_i/g_f=2$ ;<sup>1</sup>  $E(Q)\sim 0.95 \text{ eV}=1.52\times 10^{-19} \text{ J}$ ,  $\tau_Q=9.5\times 10^{-6} \text{ s}$ ; and  $E(S)\sim 0.99 \text{ eV}=1.59\times 10^{-19} \text{ J}$ ,  $\tau_S=9.5\times 10^{-6} \text{ s}$  gives total oscillator strengths,  $f_Q=6.4\times 10^{-4}$  and  $f_S=5.9\times 10^{-4}$ .  $E(Q)$  and  $E(S)$  are mean energies for the luminescence, including the phonon sidebands, assuming a Huang-Rhys factor  $S\sim 2.5$ .

An estimate can be made of the concentration of optical centers from the absorption coefficient and the oscillator strength using Smakula's equation,<sup>15</sup>

$$Nf = \frac{18m^* c \epsilon_0}{\pi e^2 \hbar} \frac{n}{(n^2+2)^2} \int \mu(E) dE, \quad (3)$$

where, in SI units, the concentration  $N$  is in  $\text{m}^{-3}$ , the absorption coefficient  $\mu$  is in  $\text{m}^{-1}$ , and the energy  $E$  is in J.

From the absorption data on the  $Q$  system in Fig. 2(a),

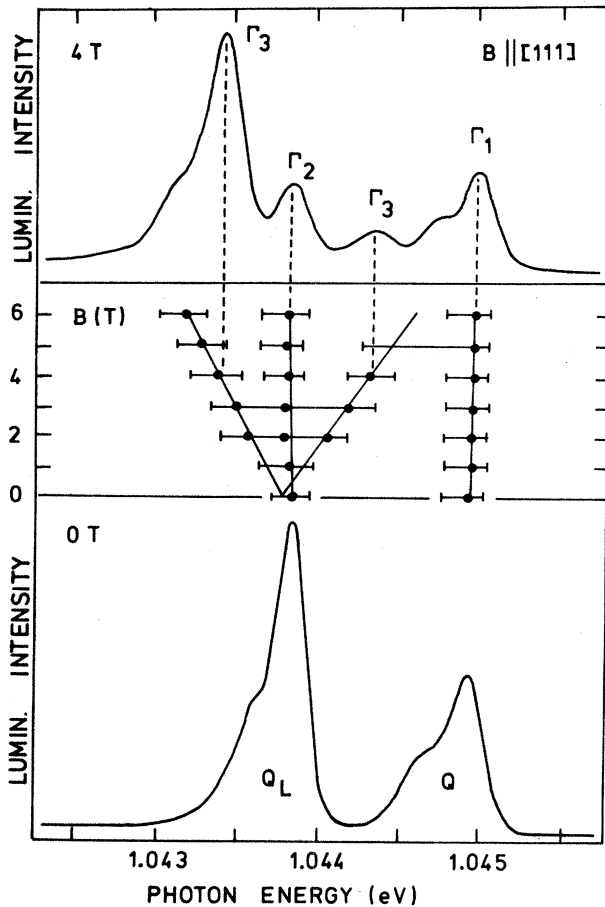


FIG. 6. Zeeman data for the  $Q$  and  $Q_L$  no-phonon lines obtained in luminescence at 2.4 K for  $\vec{B}||[111]$ . The horizontal bars indicate the full width at half maximum of the major isotropic component.

assuming that there is an underlying continuum absorption due to other sources and that the intensity of the phonon wing is negligible at  $E_{gx} + \hbar\omega(TA)$ , the integrated absorption under the phonon wing is  $\sim 3 \times 10^{-3} \text{ cm}^{-1} \text{ eV}$  compared with  $2.15 \times 10^{-4} \text{ cm}^{-1} \text{ eV}$  for the  $Q$  line and  $1.63 \times 10^{-4} \text{ cm}^{-1} \text{ eV}$  for  $Q_H$ . If it is further assumed that  $Q$  and  $Q_H$  have equal phonon coupling, the total integrated absorption due to the  $Q$  transition in this sample is  $\sim 1.9 \times 10^{-3} \text{ cm}^{-1} \text{ eV}$ . Assuming that the phonon coupling of the  $S$  line is similar to that for the  $Q$  line, for the sample used for Fig. 2(b) the integrated absorptions of the  $S$  and  $Q$  systems are  $\sim 1 \times 10^{-4}$  and  $\sim 4 \times 10^{-4} \text{ cm}^{-1} \text{ eV}$ , respectively. Substituting in Eq. (3), the concentration of  $Q$  centers in the sample used for Fig. 2(a) is  $\sim 1.8 \times 10^{15} \text{ cm}^{-3}$  and the concentrations of  $S$  and  $Q$  centers in the sample used for Fig. 2(b) are  $\sim 1 \times 10^{14}$  and  $\sim 3.7 \times 10^{14} \text{ cm}^{-3}$ , respectively. The validity of these figures is dependent on the validity of the assumptions about phonon coupling and the Lorenz local-field correction used in Smakula's equation. However, taken at face value they imply that  $< 2 \text{ wt. } \%$  of the lithium in the sample is incorporated in the  $Q$  and  $S$  optical centers.

### E. Preliminary Zeeman results

Zeeman measurements have been made on the  $Q_H$  line at  $\sim 30 \text{ K}$  and on the  $Q$  and  $Q_L$  lines between  $\sim 2.4$  and  $7.5 \text{ K}$ . Both  $Q$  and  $Q_H$  do not split, or show any appreciable shift or broadening for magnetic fields up to  $6 \text{ T}$  applied along any crystallographic direction. On the other hand, the  $Q_L$  line is clearly seen to split into three thermalizing components. Within the resolution available, the  $Q_L$  triplet splitting is completely isotropic and any zero-field splitting is  $< 0.1 \text{ meV}$ . Data for  $\vec{B}||[111]$  are shown in Fig. 6. The two outer components both shift at a rate of  $0.115 \pm 0.005 \text{ meV T}^{-1}$  which yields a  $g$  factor of  $1.99 \pm 0.08$ . In the Voigt configuration employed, none of the field-split components are completely polarized; however, the central component is strong in the  $\sigma$  spectrum and the outer components are strong in the  $\pi$  spectrum.

The triplet exciton state with an isotropic  $g$  value close to 2 and the unperturbed singlet state are most simply regarded as being formed from a spin- $\frac{1}{2}$  electron and spin- $\frac{1}{2}$  hole, the orbital angular momentum of the hole having been quenched by the axial nature of the center. The  $Q_L$  line which originates in the triplet state is weak because it is forbidden by the spin selection rule  $\Delta S=0$ . The presence of a second singlet state responsible for  $Q_H$  at higher energy suggests that there may be a set of two singlet-triplet pairs resulting from two singlet electron states being lowest in energy.<sup>7</sup> An additional stress-induced state has been observed<sup>12</sup> between  $Q$  and  $Q_H$  with a relative position similar to that of  $S^*$  in the  $S$  system no-phonon lines [Fig. 2(b)]. This could be the second triplet state, but further measurements are required before a definitive symmetry assignment can be made.

Preliminary Zeeman data have also been obtained for the two lowest energy  $S$  lines.<sup>9</sup> For  $\vec{B}||[111]$  and  $\vec{B}||[110]$ ,  $S_L$  splits into three components with  $g \sim 2$  and  $S$  does not split. However, for  $\vec{B}||[100]$  additional components are apparent which are difficult to analyze because of the presence of the isotope structure. Further measurements will be made shortly.

### IV. SUMMARY

Luminescence-decay-time measurements have confirmed the identification of the  $Q$  and  $S$  luminescence systems with exciton decay at isoelectronic defect complexes, and an estimate has been made of the concentration of these optical centers. The use of specifically carbon-doped starting material for lithium diffusion, isochronal annealing studies, and mixed isotope doping strongly suggest that the  $S$  center is, like the  $Q$  center, a four-lithium-atom complex, but one with a near-neighbor carbon atom which reinforces the trigonal symmetry. The Zeeman data suggest that both centers may be isoelectronic donors, with the hole being the more strongly bound particle, and that the axial field is sufficiently strong to decouple the orbital and spin angular momenta of the hole, giving rise to two singlet-triplet pairs of bound exciton states. A more detailed account of the uniaxial stress and Zeeman data is planned to be published elsewhere.

*Note added.* Results concerning the electronic structure of the  $\text{Li}_4$  vacancy complex has recently been published.

#### ACKNOWLEDGMENTS

We are grateful to J. G. Wilkes of Mullard Southampton for providing the carbon-doped float-zone silicon.

The work was supported by the Sciences and Engineering Research Council (SERC) and by NSERC University Research Fellowship No. UOO69. One of us (L.T.C.) was supported by a SERC Research Studentship. Another of us (M.L.W.T.) was also supported by an Alfred P. Sloan Fellowship in Basic Research.

- 
- <sup>1</sup>L. Canham, G. Davies, and E. C. Lightowers, *Physica* **117&118B**, 119 (1983).
- <sup>2</sup>M. L. W. Thewalt, U. O. Ziemelis, S. P. Watkins, and R. R. Parsons, *Can. J. Phys.* **60**, 1691 (1982); J. Wagner and R. Sauer, *Phys. Rev. B* **26**, 3502 (1982); R. Sauer and J. Weber, *Physica* **116B**, 195 (1983), and references therein.
- <sup>3</sup>N. Killoran, D. J. Dunstan, M. O. Henry, E. C. Lightowers, and B. C. Cavenett, *J. Phys. C* **15**, 6067 (1982).
- <sup>4</sup>M. L. W. Thewalt, S. P. Watkins, U. O. Ziemelis, E. C. Lightowers and M. O. Henry, *Solid State Commun.* **44**, 573 (1982).
- <sup>5</sup>P. J. Dean and D. C. Herbert, in *Excitons*, Vol. 14 of *Topics in Applied Physics*, edited by K. Cho (New York, Springer, 1979), p. 55.
- <sup>6</sup>J. W. Morgan and T. N. Morgan, *Phys. Rev. B* **1**, 739 (1970).
- <sup>7</sup>H. P. Gislason, B. Monemar, P. J. Dean, and D. C. Herbert, *Physica* **117&118B**, 269 (1983).
- <sup>8</sup>L. Canham, G. Davies, and E. C. Lightowers, *J. Phys. C* **13**, L757 (1980).
- <sup>9</sup>P. Colley and E. C. Lightowers (unpublished).
- <sup>10</sup>E. M. Pell, *J. Phys. Chem. Solids* **3**, 77 (1957).
- <sup>11</sup>L. Canham, G. Davies, and E. C. Lightowers, in *11th International Conference on Defects and Radiation Effects in Semiconductors, Oiso, 1980*, edited by R. R. Hasiguti (IOP, London, 1980), Vol. 59, p. 211.
- <sup>12</sup>L. Canham, Ph.D. thesis, University of London, 1983.
- <sup>13</sup>M. O. Henry and E. C. Lightowers, *J. Phys. C* **12**, L485 (1979).
- <sup>14</sup>K. P. O'Donnell, K. M. Lee, and G. D. Watkins, *Physica* **116B**, 258 (1983); G. Davies, E. C. Lightowers, and M. C. do Carmo, *J. Phys. C* **16**, 5503 (1983), and references therein.
- <sup>15</sup>D. L. Dexter, in *Solid State Physics*, edited by F. Seitz and D. Turnbull (Academic, New York, 1958), Vol. 6.
- <sup>16</sup>G. C. De Leo, W. B. Fowler, and G. D. Watkins, *Phys. Rev. B* **29**, 1819 (1984).